AMS

Acta Mechanica Sinica

Acta Mech. Sin.

0567-7718

1614-3116

11-2063/O3

Science Press

SP

2023

The Chinese Society of Theoretical and Applied Mechanics and Springer-Verlag GmbH Germany, part of Springer Nature

$30.00

ams2022-338

RESEARCH PAPER

Solid Mechanics

2023

Month

39

1

722338

10.1007/s10409-023-22338-x

Random dynamic responses of solar array under thermal-structural coupling based on the isogeometric analysis

Juan Ma[1,2*], Changping Dai[1,2], Bo Wang[1,2], Michael Beer[3], and Anyi Wang[1,2]

[1] Research Center of Applied Mechanics, School of Electro-Mechanical Engineering, Xidian University, Xi'an 710071, China

[2] Shaanxi Key Laboratory of Space Extreme Detection, Xidian University, Xi'an 710071 China

[3] Institute for Risk and Reliability, Faculty of Civil Engineering and Geodetic Science, Leibniz Universität Hannover, Callinstr. 34, 30900 Hannover, Germany

*Corresponding author. E-mail address: jma@xidian.edu.cn (Juan Ma)

Executive Editor: Wei Gao

Received 11 6, 2022; accepted 11 9, 2022; published online xx xx, 2023

The spacecraft experiences changes of light region periodically and will be seriously affected by the thermal stress caused by the solar radiation. Based on the isogeometric analysis, the random dynamic responses of solar array with random field parameters under thermal-structural coupling are addressed. Firstly, the heat conduction differential equation and vibration differential equation of the solar array are obtained based on the geometric model constructed with non-uniform rational B-spline. The differential equations under thermal-structural coupling are then solved by using Newmark-β method to obtain

the structural temperature field and the random dynamic responses. Finally, the influences of different random field parameters on structural dynamic response are investigated.

Random field parameters, Isogeometric analysis, Non-uniform rational B-spline, Thermal-structural coupling, Random dynamic responses

基于等几何分析的太阳帆板热结构耦合随机动力响应

马娟, 代昌平, 王博, Beer Michael, 王安意

航天器周期性地出入日光区和背光区, 会受到太阳辐射而引起周期性热应力的影响. 基于等几何分析法, 研究了具有随机场参数的太阳能帆板在热结构耦合下的随机动力响应. 首先基于非均匀有理B样条构造了帆板的几何模型, 得到太阳能帆板的热传导微分方程和振动微分方程; 利用 Newmark-β 法求解了热-结构耦合下的微分方程, 得到结构温度场和随机动力响应; 最后, 研究了不同随机场参数对结构动力响应的影响.

This work was supported by the National Natural Science Foundation of China (Grant No. 11572233) and the National Defense Pre-Research Foundation of China (Grant No. 61400020106) as well as the Fundamental Research Funds for the Central Universities.

1. Introduction

Large-scale, flexible, and low-rigidity spacecraft are popular in the space engineering [1,2]. As an important device for supplying power, the stability and reliability of solar array are of great significance for spacecraft [3,4]. When the heat caused by solar radiation exerts on the spacecraft, especially during the alternating process of the sunshine area and backlight area, the temperature gradient appears on the solar array due to the temperature difference of heat absorption between two sides of the panel, which affects the stable operation of spacecraft [5-7]. Consequently, the thermally induced vibration of solar panels occurs and further affects their reliability.

Recently, failure analysis of engineering structures in various conditions has been investigated maturely [8-12]. The thermally induced vibration of plates resulting from solar radiation has also been addressed [13]. Based on the absolute nodal coordinate method, Shen et al. [14] proposed a thermal-structural coupling model by using nonlinear finite elements (FEs) to study the thermally induced vibration of spacecraft structures subjected to thermal shock loads from solar radiation. Similarly, Pandey et al. [15] developed a FE calculation method for functionally graded material in thermally induced vibrations by using high-order layering theory, and revealed the influence of thermally induced vibration on sandwich panels. Although some progresses have been made in this literature, traditional methods such as FE analyses fail to accurately elaborate the geometric model of complicated structures, and there are still geometric approximation errors, and numerical dispersion in the solution process.

Non-uniform rational B-splines (NURBS) can effectively approximate to the geometric configuration of complicated structures with a few control points, which makes it possible to obtain high accuracy with less computation [16]. By integrating the FE model into conventional NURBS-based CAD(Computer Aided Design) design tools, the isogeometric analysis (IGA) technology has also been applied to the structural analyses [17]. Based on the IGA method, Wang et al. [18] developed a framework to solve shape optimization of transient heat conduction problems. Huynh et al. [19] adopted the IGA method to model the free vibration of beams, and the results demonstrated that the approach can represent the geometry exactly and approximate the real solution. Yang et al. [20] proposed an IGA-based PHT(Polynomial splines over Hierarchical T-meshes)-splines for crack analysis of thin-walled structures. The existing structural analyses based on the IGA method, however, mainly addressed structural static analyses or free vibration problems.

Moreover, the uncertainties of physical parameters or geometric dimensions exist objectively due to the manufacturing process [21-25]. Ma et al. [26] dealt with the random dynamic response of thin-walled tubes under thermal-structural-acoustic

coupling based on the random factor method. Currently, there also have been some works about the application of random field parameters related to the structural analysis. Arregui-Mena et al. [27] briefly reviewed the stochastic FE method related to the random field parameters or discrete random variables and introduced its application to practical problems. Scarth et al. [28] put forward a method for simulating random fields on arbitrary geometric surfaces, which addresses the fundamental issues of the defined correlation function on such surfaces as well as the subsequent evaluation in practical applications. So far, the structural dynamic response with random field parameters under multi-field coupling has not been considered.

In this work, the thermal-induced vibration of a solar array with random field parameters is investigated based on IGA to improve the analytical accuracy and to account for the uncertainties involved in modeling. The geometric model of the solar arrays seen as a plate structure is firstly constructed by using a NURBS spline surface, and the differential equations of heat conduction and dynamic differential equations are then derived by means of the IGA. Subsequently, the random analysis model of the plate is built under thermal-structural coupling by considering the physical parameters of materials as random fields. Furthermore, Newmark-β method is used to solve the differential equations to obtain the temperature field and displacement field, and the results from finite element method (FEM) and IGA are compared with each other so as to demonstrate the feasibility and validity of the model presented with IGA.

2. Random field discretization and NURBS spline function

2.1 Discretization of two-dimensional (2D) Gaussian random field

The random field coupled with FE simulations or geometric analysis can well describe the mechanical models of structures with continuously uncertain variations such as those in the mechanical properties or working loads [29-31].

The random field can be decomposed into a deterministic part $\bar{\omega}$ and a random part $\tilde{\omega}$. Based on the Karhunen-Loeve expansion [32], a 2D Gaussian random field can be expanded into a combination of orthogonal random variables $\xi_n(\theta)$ as follows:

$$\begin{aligned}\omega(x,y,\theta) &= \bar{\omega}(x,y)+\tilde{\omega}(x,y,\theta)\\ &= \bar{\omega}(x,y)+\sum_{n_1=0}^{m_1}\sum_{n_2=0}^{m_2}\sigma\cdot\xi_{n_1,n_2}(\theta)\sqrt{\lambda_n}\,f_n(x,y),\end{aligned} \tag{1}$$

where m_1 and m_2 are the truncation coefficients in the *x* and *y* directions, θ is a random event; $f_n(x,y)$ and λ_n are the eigenfunction and eigenvalue of the autocorrelation function of the random field; σ is mean square variance of the random field.

2.2 NURBS spline function

For a NURBS surface defined in the x direction with p order and in the y direction with q order, the number of basis functions is $n\times m$, and the node vectors are $\boldsymbol{U}=\{a_1,...,a_1,\xi_{p+2},...,\xi_n,b_1,...,b_1\}$ and $\boldsymbol{V}=\{a_2,...,a_2,\eta_{q+2},...,\eta_m,b_2,...,b_2\}$ in the *x* and *y* directions, respectively. Thus, the basis functions of the NURBS surface can be written as

$$
\begin{aligned}
&N_{i,p,j,q}(\xi,\eta)\\
&=\frac{B_{i,p}(\xi)B_{j,q}(\eta)\omega_{i,j}}{W(\xi,\eta)} \qquad (2)\\
&=\frac{B_{i,p}(\xi)B_{j,q}(\eta)\omega_{i,j}}{\sum_{i'=1}^{n}\sum_{j'=1}^{m}B_{i',p}(\xi)B_{j',q}(\eta)\omega_{i',j'}},
\end{aligned}
$$

where $B_{i,p}(\xi)$ and $B_{j,q}(\xi)$ are the *i*th and *j*th basis function of the rational B-spline with p and q order, respectively; $\omega_{i,j}$ is the weight of the NURBS curve[33-35].

Given $n\times m$ control points $\boldsymbol{P}_{i,j}$ ($i=1,2,...,n,\ j=1,2,...,m$), the NURBS surface $\boldsymbol{S}(\xi,\eta)$ is

$$
\boldsymbol{S}(\xi,\eta)=\sum_{i=1}^{n}\sum_{j=1}^{m}N_{i,p,j,q}(\xi,\eta)\boldsymbol{P}_{i,j}. \qquad (3)
$$

Similar to the NURBS surface, the NURBS entity, with p, q and r order in three directions, respectively, can also be obtained with $n\times m\times l$ basis functions:

$$
\begin{aligned}
&N_{i,p,j,q,k,r}(\xi,\eta,\zeta)\\
&=\frac{B_{i,p}(\xi)B_{j,q}(\eta)B_{k,r}(\zeta)\omega_{i,j,k}}{W(\xi,\eta,\zeta)} \qquad (4)\\
&=\frac{B_{i,p}(\xi)B_{j,q}(\eta)B_{k,r}(\zeta)\omega_{i,j,k}}{\sum_{i'=1}^{n}\sum_{j'=1}^{m}\sum_{k'=1}^{l}B_{i',p}(\xi)B_{j',q}(\eta)B_{k',r}(\zeta)\omega_{i',j',k'}}.
\end{aligned}
$$

3. NURBS model of plate structure

The geometric modeling of the actual structure can be accomplished with NURBS spline model and the appearance visualization can also be realized. Firstly, the characteristic lattice is collected as the control points of the spline surface according to structural configuration, then the node vector, the order of surface and the weight coefficients of control points are selected based on the number of control lattice, and the NURBS surface, can be generated with Eq. (3), as shown in Fig. 1

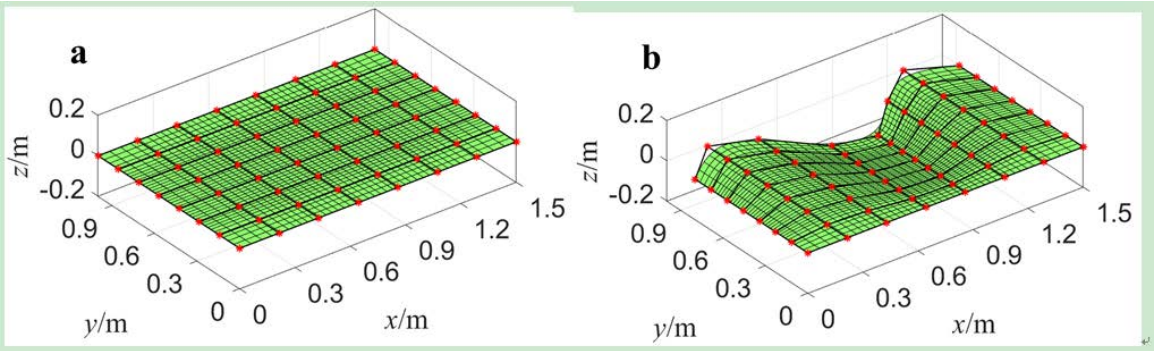

Figure 1 NURBS surfaces of the plate structure (the node vector: $\boldsymbol{U}_x = \boldsymbol{U}_y = \{0,0,0,1/6,1/3,1/2,1/3,\ 1/6,1,1,1\}$, control points: $n_x = n_y = 8\times 8$, the order: 2, the weight coefficient of control points is 1 (a); the weight coefficient of control points changes from 1 to different values (b)).

In this work, the solar array is modeled as Mindlin plate, and it is assumed that the middle surface coincides with the xOy plane in physical space. According to the property that the number of rows of control points is equal to that of columns of control points in the surface [36-38], the corresponding spline surfaces can be generated respectively when the control points of regular and irregular distribution are known.

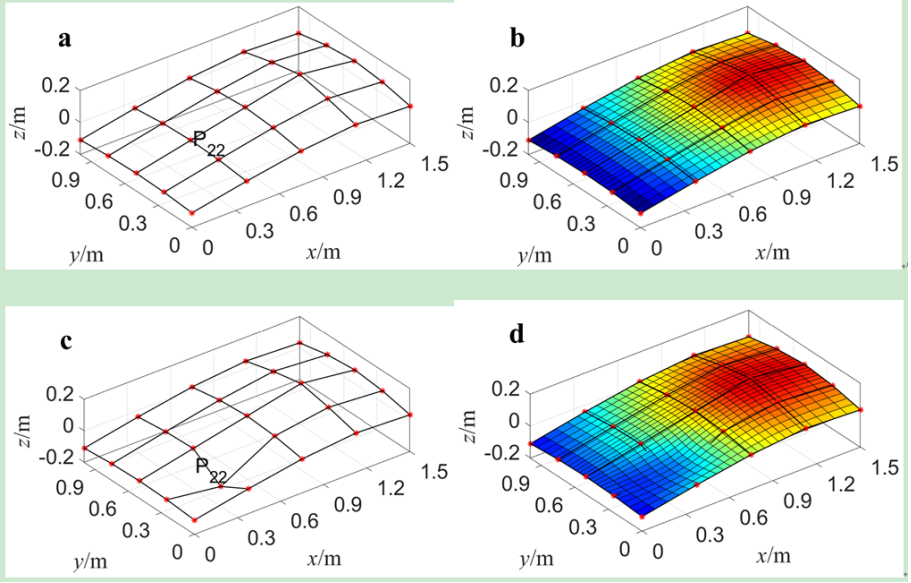

Figure 2 Adjusting NURBS surface by the movements of the control point.

When the plate experiences deformation caused by loads or the geometric model needs to be repeatedly modified, the satisfactory local modifiability by the geometric modeling with NURBS provides a possibility for IGA, and the local adjustment can change the configuration of the surface by moving the control point $\boldsymbol{P}_{i,j}$ and modifying the weight coefficient $\omega_{i,j}$, as shown in Fig. 2.

Suppose that the control point $\boldsymbol{P}_{k,l} = \boldsymbol{S}(\xi_0,\eta_0)$ moves to $\bar{\boldsymbol{P}}_{k,l}$ with a distance d along the vector $\boldsymbol{V}$, then $\bar{\boldsymbol{P}}_{k,l} = \boldsymbol{P}_{k,l} + \delta\boldsymbol{V}$, where $\delta = \dfrac{d}{|\boldsymbol{V}|N_{k,l}(\xi_0,\eta_0)}$, and $N_{k,l}(\xi_0,\eta_0)$ is the kth basis function with l order.

4. The dynamic analysis based on IGA

4.1 Stiffness matrix and mass matrix based on IGA

Isogeometric analysis is carried out by applying the isoparametric elements based on the given regular elements in local coordinate system, and then the complex elements in the physical coordinate system can be obtained through the mapping relationship. As shown in Fig 3, the physical space Ω is the real geometric model space and is expressed by the coordinate

$\boldsymbol{x}=(x,y,z)$; the parameter space $\hat{\Omega}$ is represented by the coordinate $\boldsymbol{\xi}=(\xi,\eta,\zeta)$, and it can be simplified into a multi-dimensional unit space $[0,1]^r$, where r is the dimension of space. The parent space, $\tilde{\Omega}=[-1,1]^r$, is space defined for the calculation of numerical integration.

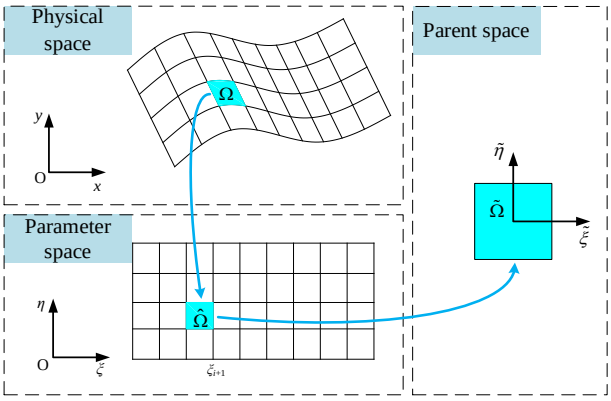

Figure 3 Spatial mapping relationship of NURBS surface.

For the basic element in NURBS parameter space $\hat{\Omega}_e=[\xi_i,\xi_{i+1}]\otimes[\eta_j,\eta_{j+1}]$, the mapping relationship in the parent domain $\tilde{\Omega}_e$ is

$$\begin{aligned}\xi&=\frac{1}{2}\left[(\xi_{i+1}-\xi_i)\tilde{\xi}+(\xi_i+\xi_{i+1})\right],\\ \eta&=\frac{1}{2}\left[(\eta_{j+1}-\eta_j)\tilde{\eta}+(\eta_j+\eta_{j+1})\right],\end{aligned}\tag{5}$$

where $\tilde{\boldsymbol{\xi}}=(\tilde{\xi},\tilde{\eta})$ denote the coordinates of parent space.

To integrate the function $f(x,y)$ in the physical space Ω, the calculation can be discretized into the basic geometric element Ω_e, and then mapped to the parameter space $\hat{\Omega}_e$ and the parent space $\tilde{\Omega}_e$, and $f(x,y)$ is then integrated via the Gauss-Legendre integration [35] as follows:

$$\begin{aligned}\int_{\Omega} f(x,y)\mathrm{d}\Omega&=\sum_{e=1}^{n}\int_{\hat{\Omega}_e} f\left[x(\xi,\eta),y(\xi,\eta)\right]\left|\boldsymbol{J}_{\xi}\right|\mathrm{d}\hat{\Omega}\\ &\approx\sum_{e=1}^{n}\sum_{i=1}^{m} f_{\tilde{\Omega}_e}\left(\tilde{\xi}_i,\tilde{\eta}_i\right)\left|\boldsymbol{J}_{\xi}\right|\left|\boldsymbol{J}_{\tilde{\xi}}\right|,\end{aligned}\tag{6}$$

where n and m are the number of elements and the number of Gauss points, $\boldsymbol{J}_{\xi}$ is the Jacobian matrix in parameter space, and $\left(\tilde{\xi}_i,\tilde{\eta}_i\right)$ is the coordinate of Gaussian integration point.

The stiffness matrix of Mindlin plate based on IGA is derived by

$$\boldsymbol{K}^{\Phi}=\iint_{A}\left[\boldsymbol{B}_{b}^{\Phi}\right]^{\mathrm{T}}\left[\boldsymbol{D}_{b}\right]\left[\boldsymbol{B}_{b}^{\Phi}\right]\mathrm{d}x\mathrm{d}y+\iint_{A}\left[\boldsymbol{B}_{s}^{\Phi}\right]^{\mathrm{T}}\left[\boldsymbol{D}_{s}\right]\left[\boldsymbol{B}_{s}^{\Phi}\right]\mathrm{d}x\mathrm{d}y,\quad(7)$$

where $\boldsymbol{D}_{b}$ and $\boldsymbol{D}_{s}$ are the elastic matrices, the bending and shear strain matrices are $\boldsymbol{B}_{b}^{\Phi}=[\boldsymbol{B}_{b11}^{\Phi}\quad\boldsymbol{B}_{b12}^{\Phi}\quad\cdots\quad\boldsymbol{B}_{bnm}^{\Phi}]$ and $\boldsymbol{B}_{s}^{\Phi}=[\boldsymbol{B}_{s11}^{\Phi}\quad\boldsymbol{B}_{s12}^{\Phi}\quad\cdots\quad\boldsymbol{B}_{snm}^{\Phi}]$, and $\boldsymbol{B}_{bij}^{\Phi}$ and $\boldsymbol{B}_{sij}^{\Phi}$ are derivative matrices of NURBS basis functions with respect to the natural coordinates:

$$\boldsymbol{B}_{bij}^{\Phi}=\begin{bmatrix}0 & 0 & \dfrac{\partial\Phi_{i,j}}{\partial x}\\ 0 & -\dfrac{\partial\Phi_{i,j}}{\partial y} & 0\\ 0 & -\dfrac{\partial\Phi_{i,j}}{\partial x} & \dfrac{\partial\Phi_{i,j}}{\partial y}\end{bmatrix},\ \boldsymbol{B}_{sij}^{\Phi}=\begin{bmatrix}\dfrac{\partial\Phi_{i,j}}{\partial y} & -\Phi_{i,j} & 0\\ \dfrac{\partial\Phi_{i,j}}{\partial x} & 0 & \Phi_{i,j}\end{bmatrix},\quad(8)$$

where $\Phi_{i,j}$ is 2D NURBS basis function used as the shape function in IGA.

Similar to the element mass matrix derived from FEM, the isogeometric mass matrix of Mindlin plate can be obtained with the consistent mass matrix:

$$\boldsymbol{M}^{\Phi}=\iiint_{V}\rho\boldsymbol{\Phi}_{\mathrm{s}}^{\mathrm{T}}\boldsymbol{\Phi}_{\mathrm{s}}\mathrm{d}V,\qquad(9)$$

$$\boldsymbol{\Phi}_{s}=\left[\boldsymbol{\Phi}_{s11}\quad\boldsymbol{\Phi}_{s12}\quad\cdots\quad\boldsymbol{\Phi}_{snm}\right],$$
$$\boldsymbol{\Phi}_{sij}=\begin{bmatrix}0 & 0 & -z\Phi_{i,j}\\ 0 & z\Phi_{i,j} & 0\\ \Phi_{i,j} & 0 & 0\end{bmatrix},\quad(10)$$
$$\left(i=1,2,\cdots,n;\ \ j=1,2,\cdots,m\right)$$

where $\boldsymbol{\Phi}_{s}$ is the NURBS basis function matrix; z represents the coordinates in the thickness direction of the plate.

Subsequently, the proportional damping matrix can be obtained by combining the isogeometric stiffness matrix and the mass matrix, as

$$\boldsymbol{C}^{\Phi}=\alpha_{r}\boldsymbol{M}^{\Phi}+\beta_{r}\boldsymbol{K}^{\Phi},\quad(11)$$

where α_{r} and β_{r} are constants to be determined.

For a single NURBS surface, it is not necessary to assemble the global matrices, and the kinetic equation of the structure based on IGA is

$$\left[\boldsymbol{M}^{\Phi}\right]\left\{\ddot{\boldsymbol{d}}\right\}+\left[\boldsymbol{C}^{\Phi}\right]\left\{\dot{\boldsymbol{d}}\right\}+\left[\boldsymbol{K}^{\Phi}\right]\left\{\boldsymbol{d}\right\}=\left\{\boldsymbol{P}^{\Phi}\right\}, \quad (12)$$

where $\{\boldsymbol{d}\}$, $\left\{\dot{\boldsymbol{d}}\right\}$ and $\left\{\ddot{\boldsymbol{d}}\right\}$ are structural displacement, velocity and acceleration, $\left\{\boldsymbol{P}^{\Phi}\right\}$ is the equivalent load on the structural control points.

4.2 Thermal equation based on IGA

In this work, the thermal equation is derived on the heat conduction element of the plate by using IGA, and the dimensions of the element are $a \gg h$ and $b \gg h$, as shown in Fig. 4. The element is only affected by radiation heat transfer and heat conduction according to the solar array in space, and two assumptions are made: (1) only heat absorption due to sunlight radiation as well as radiation heat dissipation from A_1 and A_2 surfaces are considered; (2) the average temperature of plate is much higher than the temperature difference, and thermal stress is supposed to be induced by temperature difference.

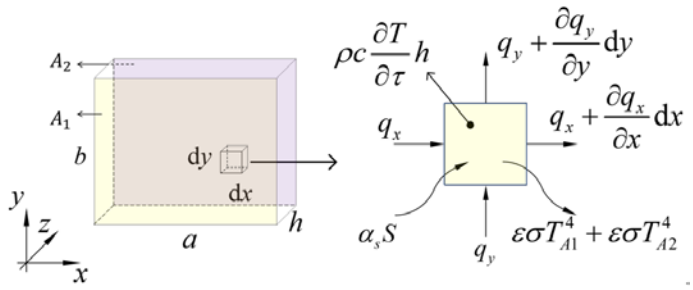

Figure 4 Heat conduction of the plate.

The heating and heat flux density can be analyzed by taking the infinitesimal element $\mathrm{d}x \times \mathrm{d}y \times h$ in the plate element in Fig. 4, in which heat flux like q_x in x, y and z directions, heat flux input $\alpha_s S$ of surface A_1 irradiated by the sun, and heat flux output like $\varepsilon\sigma AT^4$ generated by radiation and heat dissipation of A_1 and A_2 surfaces are included. According to Fourier law and energy conservation, the differential equation of heat conduction can be obtained:

$$\frac{\partial q_x}{\partial x}+\frac{\partial q_y}{\partial y}+\frac{\partial q_z}{\partial z}+\rho c\frac{\partial T}{\partial \tau}+q_0=0, \quad (13)$$

where q_0 is the heating capacity of the heat source inside the structure, hereby q_0 = 0; ρ and c are the mass density and specific heat capacity; T and τ are the temperature field and the time variable, q_x, q_y and q_z are the heat flux in three directions. The heat flux and temperature field meet $q_x=-k_x\frac{\partial T}{\partial x}$, $q_y=-k_y\frac{\partial T}{\partial y}$, $q_z=-k_z\frac{\partial T}{\partial z}$, and k_x, k_y and k_z denote the coefficient of thermal conductivity in three directions.

Then, the heat balance equation is then derived as

$$-\frac{\partial}{\partial x}\left(k_x\frac{\partial T}{\partial x}\right)-\frac{\partial}{\partial y}\left(k_y\frac{\partial T}{\partial y}\right)-\frac{\partial}{\partial z}\left(k_z\frac{\partial T}{\partial z}\right)+\rho c\frac{\partial T}{\partial \tau}=0. \quad (14)$$

The relationship between the normal vector $\boldsymbol{n}$ and the radiant heat flux $\boldsymbol{S}_0$ of sunlight is illustrated in Fig. 5, and the net radiant heat flux on the surface of the plate is

$$S=S_0\frac{-\boldsymbol{n}\cdot\boldsymbol{s}}{|-\boldsymbol{n}||\boldsymbol{s}|}=\frac{-\boldsymbol{n}\cdot\boldsymbol{S}_0}{|-\boldsymbol{n}||\boldsymbol{S}_0|}, \quad (15)$$

where $\boldsymbol{s}$ is the direction vector of solar thermal radiation.

From Fig. 4, when considering the absorption of the heat of solar radiation and heat dissipation in space, the boundary condition of the plate is

$$\frac{\partial q_z}{\partial z}\boldsymbol{n}_z=\alpha_s S_0\frac{-\boldsymbol{n}\cdot\boldsymbol{s}}{|-\boldsymbol{n}||\boldsymbol{s}|}-\varepsilon\sigma T_{A_1}^4-\varepsilon\sigma T_{A_2}^4. \quad (16)$$

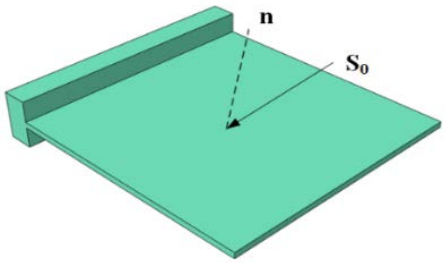

Figure 5 Heat flux absorbed by structure.

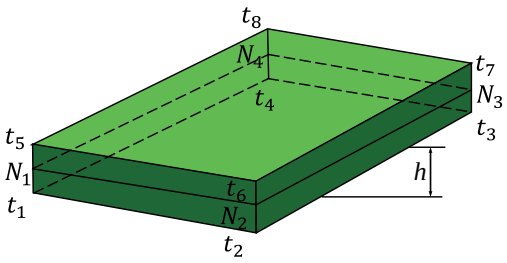

Figure 6 3D plate element.

To consider the three-dimensional (3D) heat balance equation of solar array based on IGA, the 2D plate element is extended to the 3D condition in Fig. 6. *h* is the thickness of the element, and N_1-N_4 are the four nodes on the neutral layer of the plate element, and the corresponding coordinates is $(x_1,y_2,0)$-$(x_4,y_4,0)$; t_1-t_8 represent eight nodes of heat conduction element.

The heat conduction in Eq. (14) should be expressed by the 3D NURBS basis functions. So the 2D NURBS surface should be extended to 3D one with IGA, and the plate is then extended by a distance of *h*/2 in the positive and negative directions of the thickness so as to describe the temperature field.

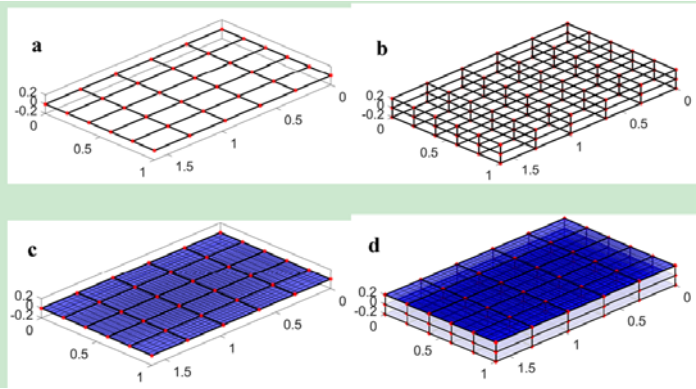

Figure 7 Temperature field of NURBS 3D entity.

In Fig. 7, the plate, with the length <♥>1.6♣m,</♥> the width <♥>1♣m</♥> and the thickness <♥>0.4♣m,</♥> is modeled with 2D NURBS surface to represent the neutral surface in the IGA. Figure 7a shows the control points and grid. When the control points on the neutral surface are respectively moved upward and down <♥>0.2♣m,</♥> Fig. 7b shows the control points and control grid of NURBS entity. When the order in each direction of 2D NURBS basis function is 2 and the weight coefficient of control points is 1, the spline surface is shown in Fig. 7c, similarly, when NURBS basis function with the weight coefficient 1.0 for every control point is chosen, the NURBS entity is shown in Fig. 7d.

Then the temperature field of the plate under IGA analysis in Eq. (16) can be expressed as

$$T\left(x,y,z,\tau\right)=\sum_{i=1}^{n}\sum_{j=1}^{m}\sum_{k=1}^{l}\Phi_{i,j,k}^{\mathrm{T}}\left(\xi,\eta,\zeta\right)\boldsymbol{T}_{e}\left(\tau\right)=\boldsymbol{\Phi}^{\mathrm{T}}\left(\xi,\eta,\zeta\right)\boldsymbol{T}\left(\tau\right),\qquad(17)$$

where $\boldsymbol{T}\left(\tau\right)$ is the temperature vector of control points at any time, $\Phi_{i,j,k}^{\mathrm{T}}\left(\xi,\eta,\zeta\right)$ $\left(l\le i\le n,\ l\le j\le m,\ l\le k\le l\right)$ is the 3D NURBS basis function and $\boldsymbol{\Phi}^{\mathrm{T}}\left(\xi,\eta,\zeta\right)$ is the basis function matrix.

According to Eqs. (14) and (15), the heat balance equation is integrated in the element by using Galerkin method:

$$\underbrace{\int_{V}\left(k_{x}\left[\frac{\partial\boldsymbol{\Phi}_{T}}{\partial x}\right]^{\mathrm{T}}\left[\frac{\partial\boldsymbol{\Phi}_{T}}{\partial x}\right]+k_{y}\left[\frac{\partial\boldsymbol{\Phi}_{T}}{\partial y}\right]^{\mathrm{T}}\left[\frac{\partial\boldsymbol{\Phi}_{T}}{\partial y}\right]+k_{z}\left[\frac{\partial\boldsymbol{\Phi}_{T}}{\partial z}\right]^{\mathrm{T}}\left[\frac{\partial\boldsymbol{\Phi}_{T}}{\partial z}\right]\right)\mathrm{d}V}_{\boldsymbol{k}_{t}^{\Phi}}T^{4}+\underbrace{\int_{V}\rho C\boldsymbol{\Phi}_{T}^{\mathrm{T}}\boldsymbol{\Phi}_{T}\mathrm{d}V}_{\boldsymbol{C}_{t}^{\Phi}}\dot{T}_{e}$$
$$=\underbrace{-\oint_{\Gamma}\left(q_{x}\boldsymbol{n}_{x}+q_{y}\boldsymbol{n}_{y}\right)\mathrm{d}\Gamma}_{\boldsymbol{Q}_{0}}+\underbrace{\int_{A_{1}}\boldsymbol{\Phi}_{T}^{\mathrm{T}}\alpha_{s}S_{0}\frac{-\boldsymbol{n}\cdot\boldsymbol{s}}{\left|-\boldsymbol{n}\right|\left|\boldsymbol{s}\right|}\mathrm{d}A}_{\boldsymbol{Q}_{q0}}-\underbrace{\int_{A_{1}}\boldsymbol{\Phi}_{T}^{\mathrm{T}}\varepsilon\sigma T_{A_{1}}^{4}\mathrm{d}A}_{R_{A_{1}}}-\underbrace{\int_{A_{2}}\boldsymbol{\Phi}_{T}^{\mathrm{T}}\varepsilon\sigma T_{A_{2}}^{4}\mathrm{d}A}_{R_{A_{2}}}.\qquad(18)$$

Thus, the heat balance equation in the element, i.e. Eq. (18), is further simplified by

$$\boldsymbol{K}_{T}^{\Phi}\boldsymbol{T}+\boldsymbol{C}_{T}^{\Phi}\dot{\boldsymbol{T}}=\boldsymbol{Q}_{q}-\boldsymbol{R}_{A_{1}}-\boldsymbol{R}_{A_{2}},\qquad(19)$$

where $\boldsymbol{C}_T^{\Phi}$ is the isogeometric heat capacity matrix, $\boldsymbol{K}_T^{\Phi}$ is the isogeometric thermal stiffness matrix, $\boldsymbol{Q}_q$ is the input of solar heat flux, $\boldsymbol{R}_{A_1}$ and $\boldsymbol{R}_{A_2}$ are the radiation heat dissipation of upper and lower surfaces. Since the equivalent thermal loads inside the plate cancel each other, $\boldsymbol{Q}_0 = 0$.

4.3 The IGA model of structures with random field parameters

Given the mean value $\overline{E}$ of elastic modulus E of the plate, the coefficient of variation CV_E and the correlation lengths L_x and L_y, the elastic modulus random field can be expressed from Eq. (1) as

$$E(x,y,\theta) = \overline{E} + \sum_{n_1=0}^{m_1}\sum_{n_2=0}^{m_2} \sigma_E \xi_{n_1,n_2}(\theta)\sqrt{\lambda_{n_1}\cdot\lambda_{n_2}}\, f_{n_1}(x)\cdot f_{n_2}(y). \quad (20)$$

Similarly, the structural mass density ρ is considered as a 2D random field parameter, which can be written by

$$\rho(x,y,\theta) = \overline{\rho} + \sum_{n_1=0}^{m_1}\sum_{n_2=0}^{m_2} \sigma_\rho \xi_{n_1,n_2}(\theta)\sqrt{\lambda_{n_1}\cdot\lambda_{n_2}}\, f_{n_1}(x)\cdot f_{n_2}(y), \quad (21)$$

where $\overline{\rho}$ is the mean value of ρ, and standard deviation $\sigma_\rho = CV_\rho \cdot \overline{\rho}$.

For the plate structure under thermal-structural coupling, the random stiffness matrix is obtained by using the random field model and IGA, as

$$\tilde{\boldsymbol{K}}^{\Phi} = \overline{\boldsymbol{K}}^{\Phi} + \sum_{n_1=0}^{m_1}\sum_{n_2=0}^{m_2} \boldsymbol{K}_{n_1,n_2}^{\Phi}\xi_{n_1,n_2}(\theta), \quad (22)$$

where the mean isogeometric stiffness matrix $\overline{\boldsymbol{K}}^{\Phi}$ and the random matrix $\boldsymbol{K}_{n_1,n_2}^{\Phi}$ are

$$\overline{\boldsymbol{K}}^{\Phi} = \iint_A \left[\boldsymbol{B}_b^{\Phi}\right]^{\mathrm{T}}\left[\boldsymbol{D}_b\right]\left[\boldsymbol{B}_b^{\Phi}\right]\mathrm{d}x\mathrm{d}y + \iint_A \left[\boldsymbol{B}_s^{\Phi}\right]^{\mathrm{T}}\left[\boldsymbol{D}_s\right]\left[\boldsymbol{B}_s^{\Phi}\right]\mathrm{d}x\mathrm{d}y, \quad (23)$$

$$\begin{aligned}\boldsymbol{K}_{n_1,n_2}^{\Phi} = \sigma_E\sqrt{\lambda_{n_1}\cdot\lambda_{n_2}}\Big[&\int_A f_{n_1}(x)\cdot f_{n_2}(y)\boldsymbol{\Phi}_s^{\mathrm{T}}\boldsymbol{D}_b\boldsymbol{\Phi}_s\mathrm{d}x\mathrm{d}y \\ &+\int_A f_{n_1}(x)\cdot f_{n_2}(y)\boldsymbol{\Phi}_s^{\mathrm{T}}\boldsymbol{D}_s\boldsymbol{\Phi}_s\mathrm{d}x\mathrm{d}y\Big].\end{aligned} \quad (24)$$

Accordingly, the random isogeometric mass matrix based on random field is

$$\tilde{\boldsymbol{M}}^{\Phi} = \overline{\boldsymbol{M}}^{\Phi} + \sum_{n_1=0}^{m_1}\sum_{n_2=0}^{m_2} \boldsymbol{M}_{n_1,n_2}^{\Phi}\xi_{n_1,n_2}(\theta), \quad (25)$$

where $\bar{\boldsymbol{M}}^{\Phi}$ is the mean isogeometric mass matrix, the random matrix $\boldsymbol{M}_{n_1,n_2}^{\Phi}$ is

$$\boldsymbol{M}_{n_1,n_2}^{\Phi}=\sigma_{\rho}\sqrt{\lambda_{n_1}\cdot\lambda_{n_2}}\int_A f_{n_1}(x)\cdot f_{n_2}(y)\boldsymbol{\Phi}_s^{\mathrm{T}}\boldsymbol{\Phi}_s\mathrm{d}x\mathrm{d}y. \quad (26)$$

4.4 The random dynamic response of plate under thermal-structural coupling based on IGA

With the temporal difference method and Newton's inner iteration, the recurrence formula of Eq. (19) can be obtained:

$$\begin{aligned}&\left(2\boldsymbol{K}_T^{\Phi}+3\boldsymbol{C}_T^{\Phi}/\Delta t\right)\boldsymbol{T}_{t+\Delta t}\\&=\left(3\boldsymbol{C}_T^{\Phi}/\Delta t-\boldsymbol{K}_T^{\Phi}\right)\boldsymbol{T}_t+3\left(\boldsymbol{Q}_q-\boldsymbol{R}_{A_1}-\boldsymbol{R}_{A_2}\right).\end{aligned} \quad (27)$$

The differential equations of the structure are then expanded by adopting the Newmark-β method [39-41]:

$$\begin{cases}\tilde{\boldsymbol{K}}\boldsymbol{d}_{t+\Delta t}=\tilde{\boldsymbol{P}}_{t+\Delta t},\\ \ddot{\boldsymbol{d}}_{t+\Delta t}=a_0\left(\boldsymbol{d}_{t+\Delta t}-\boldsymbol{d}_t\right)-a_2\dot{\boldsymbol{d}}_t-a_3\ddot{\boldsymbol{d}}_t,\\ \dot{\boldsymbol{d}}_{t+\Delta t}=\dot{\boldsymbol{d}}_t+a_6\ddot{\boldsymbol{d}}_t+a_7\ddot{\boldsymbol{d}}_{t+\Delta t},\end{cases} \quad (28)$$

where $\boldsymbol{d}$ is the displacement of control points, and the displacement of any point in an element is $\boldsymbol{u}=\boldsymbol{\Phi}\boldsymbol{d}$; $\tilde{\boldsymbol{K}}$ and $\tilde{\boldsymbol{P}}_{t+\Delta t}$ are random equivalent stiffness matrix and random equivalent load, and

$$\tilde{\boldsymbol{K}}=\tilde{\boldsymbol{K}}^{\Phi}+a_0\tilde{\boldsymbol{M}}^{\Phi}+a_1\boldsymbol{C}^{\Phi} \quad (29)$$

$$\begin{aligned}\tilde{\boldsymbol{P}}_{t+\Delta t}=&\tilde{\boldsymbol{P}}_{t+\Delta t}^{\Phi}+\tilde{\boldsymbol{M}}^{\Phi}\left(a_0\boldsymbol{d}_i+a_2\dot{\boldsymbol{d}}_i+a_3\ddot{\boldsymbol{d}}_i\right)\\&+\boldsymbol{C}^{\Phi}\left(a_1\boldsymbol{d}_i+a_4\dot{\boldsymbol{d}}_i+a_5\ddot{\boldsymbol{d}}_i\right),\end{aligned} \quad (30)$$

where the random temperature load $\tilde{\boldsymbol{P}}_{t+\Delta t}^{\Phi}=\tilde{\boldsymbol{P}}_T=\sum_e\int_{A^e}\begin{bmatrix}\boldsymbol{B}_b\\ \boldsymbol{B}_s\end{bmatrix}^{\mathrm{T}}\boldsymbol{D}\boldsymbol{K}_T\mathrm{d}x\mathrm{d}y$ can be computed after solving the temperature field according to Eq. (27).

Given the time step, the integration parameters in Newmark-β method are set as $\gamma=0.5$ and $\beta=0.25$, the random dynamic response under thermal-structural coupling can be obtained by iterative calculation based on Eqs. (27) and (28), and the structural stress can also be computed according to the relationship between the displacement of element control points and the stress of the element based on IGA.

5. Numerical example

The solar panel is considered as a plate and the material parameters are listed in Table 1. When the spacecraft moves from the shadow area to the lighting area, the period $t=0\text{-}500$ s corresponds to the sudden illuminations applied to the solar panel. The heat flux density of sunlight is $S_0=1350\ \mathrm{W\,m^{-2}}$, the initial temperature is $T_0=290$ K, and the iteratively computing time interval $\Delta t=0.1$ s.

Table 1 Structural parameters

Elastic modulus $E\ (\mathrm{GPa})$	Density $\rho\ (\mathrm{kg/m^3})$	Thickness $h\ (\mathrm{m})$	Specific heat capacity $c\ (\mathrm{J\,kg^{-1}\,K^{-1}})$	Poisson's ratio μ
1.242	1.32×10^3	0.005	1.1×10^3	0.4
Thermal conductivity $k\ (\mathrm{W\,m^{-1}\,K^{-1}})$	Thermal expansion coefficient $\alpha\ (\mathrm{K^{-1}})$	Outer surface heat absorption coefficient α_s	Surface heat dissipation coefficient ε	
0.5	1.85×10^{-4}	0.5	0.2	

Based on IGA, the order of NURBS spline surface is $p=q=2$, the node vectors in x and y directions are $\boldsymbol{U}_\eta$ = {0, 0, 0, 0.14, 0.29, 0.43, 0.57, 0.71, 0.86, 1, 1, 1} and $\boldsymbol{U}_\xi$ = {0, 0, 0, 0.08, 0.15, 0.23, 0.31, 0.38, 0.46, 0.54, 0.62, 0.69, 0.77, 0.85, 0.92, 1, 1, 1}. Figure 8 is the displacement distribution with different numbers of control points.

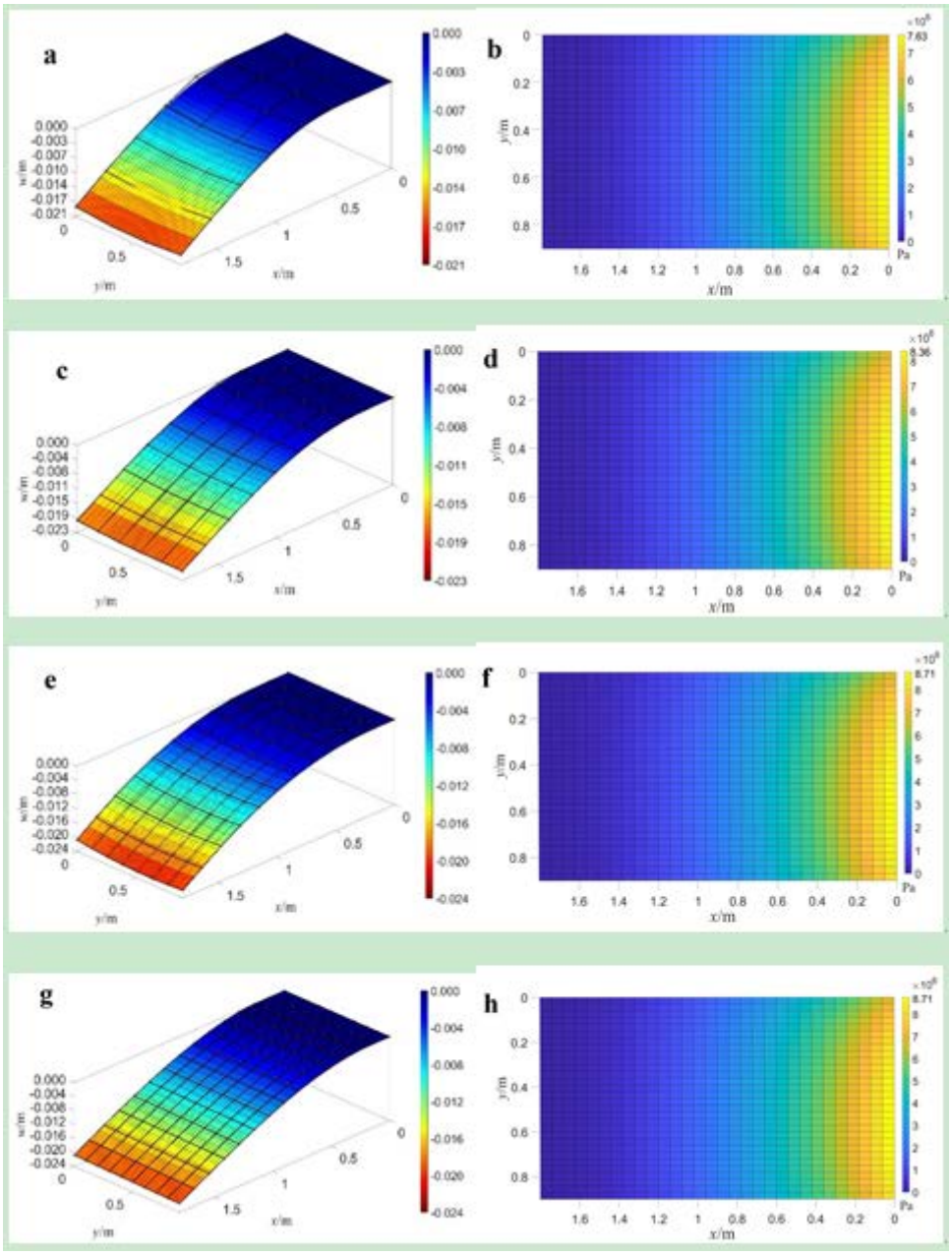

Figure 8 Displacement distribution in the plate under thermal-structural coupling.

As can be seen from Fig. 8, the displacement in the plate tends to converge with the increase of the number of control points, so the number of control points is selected as $n_x \times n_y = 12 \times 8$ in the following computation with the consideration of computational cost and the accuracy.

Suppose that Young's modulus E and mass density ρ of the material are considered as random fields as listed in Table 2.

Table 2 Random field parameters

Random field	Mean	CV	*x*-axis correlation length (m)	*y*-axis correlation length (m)
E	$\mu_E = 1.242$ GPa	0.02	0.3	0.3
ρ	$\mu_\rho = 1.32 \times 10^3$ kg m^{-3}	0.02	0.3	0.3

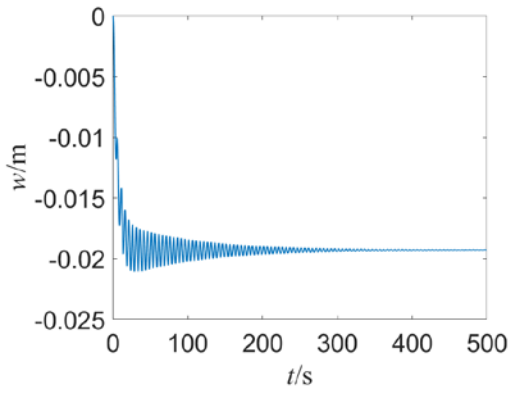

Figure 9 Maximum displacement.

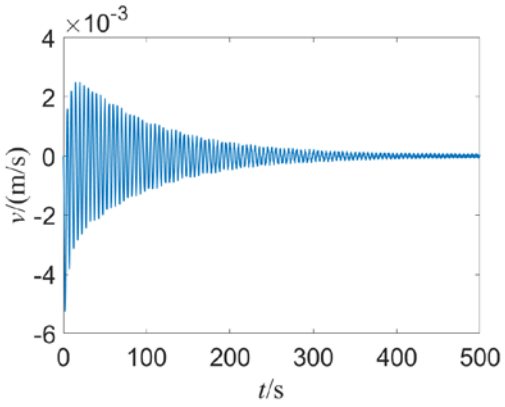

Figure 10 Corresponding speed.

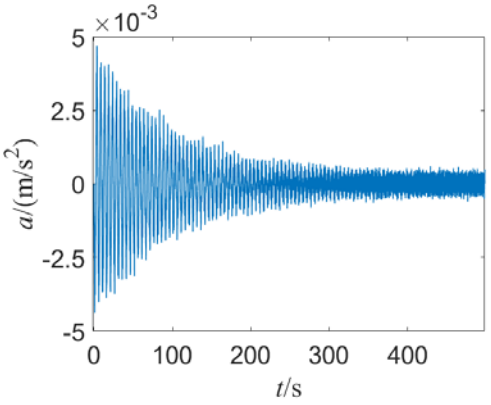

Figure 11 Corresponding acceleration.

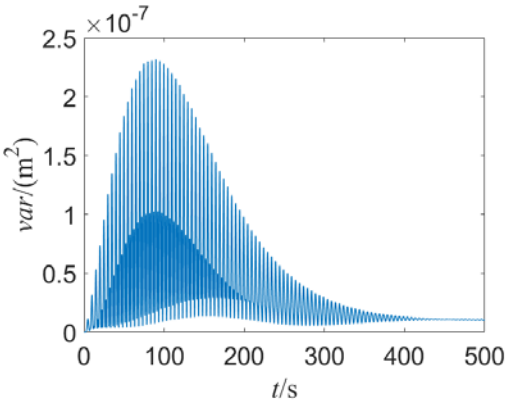

Figure 12 Variance of maximum displacement.

The time-histories of mean of the maximum displacement in the plate, and of the corresponding velocity and acceleration are illustrated in Figs. 9-11. The vibration amplitude of the spacecraft in the first <♥>200♣s</♥> is the greatest after the spacecraft enters the sunlight.

Based on the random thermal-structural coupling model and NURBS geometric model, 1000 sets of samples of E and ρ are used to calculate the variance of the maximum displacement. The result in Fig. 12 displays that the randomness of physical parameters has a great influence on the structural vibration, and the effect is reduced as the vibration tends to be stable.

The results of thermal-structural coupling computed with FEM and IGA are compared as shown in Fig. 13, and they are close to each other.

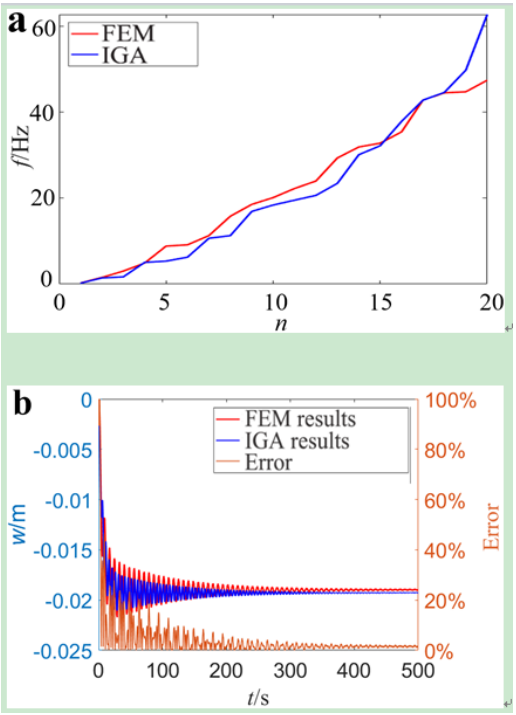

Figure 13 Results computing with two methods: **a** the comparison of natural frequency and **b** that of maximum displacement.

To investigate the influence of random field parameters on structural vibration responses, the correlation lengths of both

E and ρ are taken as $L_x = L_y = 0.3$ m, and the coefficients of variation CV_E and CV_ρ are taken as different values. The mean and variance of the dynamic response are computed by FEM and IGA in the first <♥>200♣s</♥> as illustrated in Fig. 14, and 500 samples are extracted for each group of random field parameters.

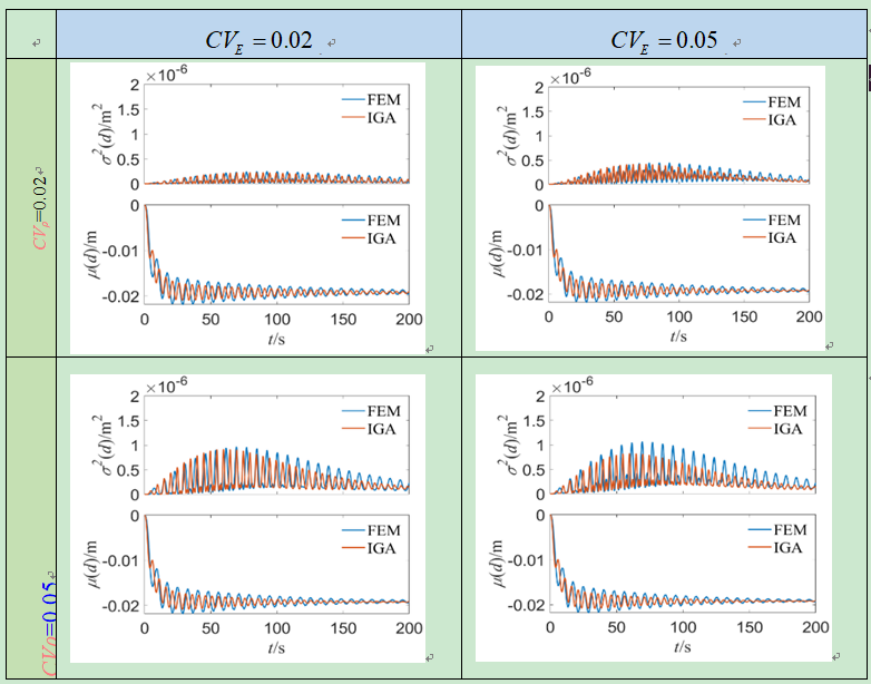

Figure 14 Mean and variance of maximum displacement with different CV_E and CV_ρ.

As can be seen from Fig. 14, CV_E and CV_ρ have an obvious effect on the variance of displacement response, in which the former has a greater influence on the uncertainty of the dynamic response than the latter.

In the following, given the coefficients of variation and the correlation length in *y* direction of E and ρ, i.e., $CV_E = CV_\rho = 0.05$, $L_{Ey} = L_{\rho y} = 0.3$ m, while the correlation lengths of E and ρ in *x* direction are taken as different groups. 500 samples are used to calculate the dynamic displacement within <♥>200♣s,</♥> and the mean and variance of the response are illustrated in Fig. 15.

From Figs. 14 and 15, it appears that acceptable differences exist in the results obtained by FEM and IGA, but the trend of the mean and variance of the dynamic responses from two methods are the same, which displays the feasibility and validity of the model presented with IGA. Compared to CV_ρ, CV_E affects more the dynamic response. The correlation length L_{Ex} and $L_{\rho x}$ do not greatly affect the randomness of the dynamic response of the plate, and the randomness of dynamic responses more results from CV_E and CV_ρ, that is, the variance of the dynamic response is great in Fig. 15 because CV_ρ and CV_E are set a large value, as 0.05.

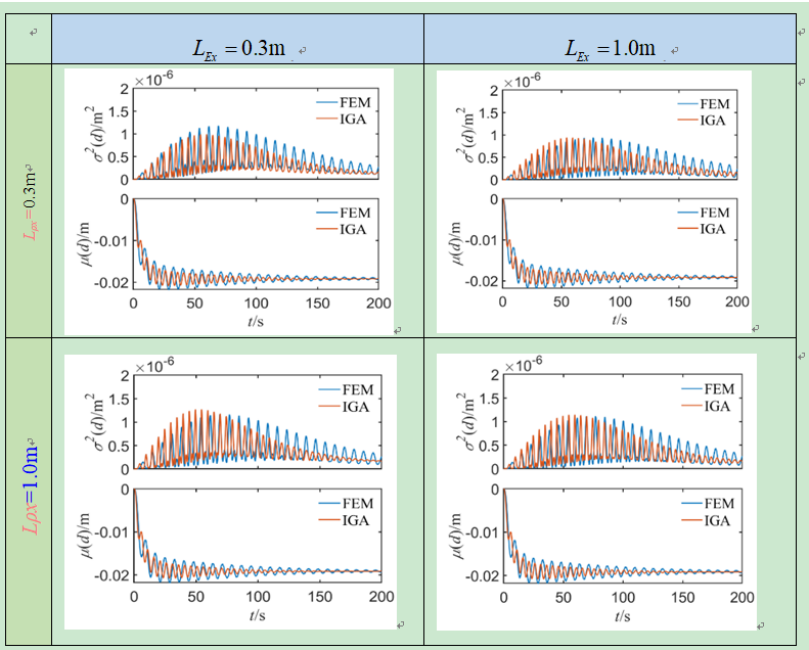

Figure 15 Mean and variance of maximum displacement with different L_{Ex} and $L_{\rho x}$.

6. Conclusions

In this work, a solar panel is considered as a Mindlin plate under thermal-structural coupling, and the dynamic response is numerically analyzed with IGA by modeling the plate with NURBS spline surfaces. Initially, the heat conduction differential equation and dynamic differential equation are established respectively based on IGA after refining the NURBS model. The numerical calculation is then carried out in the time domain to obtain the temperature field and displacement field of the structure. Finally, the statistical results of the structural displacement response are obtained by sampling and analyzing the random field parameters of different physical variables. When considering Young's modulus and mass density as random fields, the uncertainty of the former holds a greater impact on the dynamic response of the plate structure than that of the latter. Furthermore, the coefficient of variation of the random fields exerts a greater effect on the results than the correlation length does, which can provide guidance for the design and material selection of solar panel structure.

Juan Ma designed and perform the research. Changping Dai, Bo Wang and Anyi Wang wrote the first draft of the manuscript. Michel Beer helped to design the example, organize and revise the manuscript.

This work was supported by the National Natural Science Foundation of China (Grant No. 11572233) and the National Defense Pre-Research Foundation of China (Grant No. 61400020106) as well as the Fundamental Research Funds for the Central Universities.

1. <r>\author{<a><g>J.</g><s>Wei</s><a><g>D.</g><s>Cao</s><a><g>L.</g><s>Wang</s><a><g>H.</g><s>Huang</s><a><g>W.</g><s>Huang</s>}, \title{Dynamic modeling and simulation for flexible spacecraft with flexible jointed solar panels}, \journal{Int. J. Mech. Sci.}, \year{2017}, \vol{130}, \fpage{558}, \doi{10.1016/j.ijmecsci.2017.06.037}</r>

2. <r>\author{<a><g>H.</g><s>Li</s><a><g>H. Z.</g><s>Huang</s><a><g>Y. F.</g><s>Li</s><a><g>J.</g><s>Zhou</s><a><g>J.</g><s>Mi</s>}, \title{Physics of failure-based reliability prediction of turbine blades using multi-source information fusion}, \journal{Appl. Soft Comput.}, \year{2018}, \vol{72}, \fpage{624}, \doi{10.1016/j.asoc.2018.05.015}</r>

3. <r>\author{<a><g>Y.</g><s>Cao</s><a><g>D.</g><s>Cao</s><a><g>G.</g><s>He</s><a><g>L.</g><s>Liu</s>}, \title{Thermal alternation induced vibration analysis of spacecraft with lateral solar arrays in orbit}, \journal{Appl. Math. Model.}, \year{2020}, \vol{86}, \fpage{166}, \doi{10.1016/j.apm.2020.05.008}</r>

4. <r>\author{<a><g>P. G. V.</g><s>Sampaio</s><a><g>M. O. A.</g><s>González</s>}, \title{Photovoltaic solar energy: conceptual framework}, \journal{Renew. Sustain. Energy Rev.}, \year{2017}, \vol{74}, \fpage{590}, \doi{10.1016/j.rser.2017.02.081}</r>

5. <r>\author{<a><g>J.</g><s>Li</s><a><g>S.</g><s>Yan</s>}, \title{Thermally induced vibration of composite solar array with honeycomb panels in low earth orbit}, \journal{Appl. Thermal Eng.}, \year{2014}, \vol{71}, \fpage{419}, \doi{10.1016/j.applthermaleng.2014.07.015}</r>

6. <r>\author{<a><g>H.</g><s>Li</s><a><g>Z. M.</g><s>Deng</s><a><g>N. A.</g><s>Golilarz</s><a><g>C.</g><s>Guedes Soares</s>}, \title{Reliability analysis of the main drive system of a CNC machine tool including early failures}, \journal{Reliab. Eng. Syst. Saf.}, \year{2021}, \vol{215}, \fpage{107846}, \doi{10.1016/j.ress.2021.107846}</r>

7. <r>\author{<a><g>J.</g><s>Li</s><a><g>S.</g><s>Yan</s><a><g>R.</g><s>Cai</s>}, \title{Thermal analysis of composite solar array subjected to space heat flux}, \journal{Aerosp. Sci. Tech.}, \year{2013}, \vol{27}, \fpage{84}, \doi{10.1016/j.ast.2012.06.010}</r>

8. <r>\author{<a><g>H.</g><s>Li</s><a><g>C.</g><s>Guedes Soares</s><a><g>H. Z.</g><s>Huang</s>}, \title{Reliability analysis of a floating offshore wind turbine using Bayesian Networks}, \journal{Ocean Eng.}, \year{2020}, \vol{217}, \fpage{107827}, \doi{10.1016/j.oceaneng.2020.107827}</r>

9. <r>\author{<a><g>P.</g><s>Yue</s><a><g>J.</g><s>Ma</s><a><g>H.</g><s>Huang</s><a><g>Y.</g><s>Shi</s><a><g>J. W.</g><s>Zu</s>}, \title{Threshold damage-based fatigue life prediction of turbine blades under combined high and low cycle fatigue}, \journal{Int. J. Fatigue}, \year{2021}, \vol{150}, \fpage{106323}, \doi{10.1016/j.ijfatigue.2021.106323}</r>

10. <r>\author{<a><g>H.</g><s>Li</s><a><g>H.</g><s>Díaz</s><a><g>C.</g><s>Guedes Soares</s>}, \title{A failure analysis of floating offshore wind turbines using AHP-FMEA methodology}, \journal{Ocean Eng.}, \year{2021}, \vol{234}, \fpage{109261}, \doi{10.1016/j.oceaneng.2021.109261}</r>

11. <r>\author{<a><g>H.</g><s>Li</s><a><g>A. P.</g><s>Teixeira</s><a><g>C.</g><s>Guedes Soares</s>}, \title{A two-stage failure mode and effect analysis of offshore wind turbines}, \journal{Renew. Energy}, \year{2020}, \vol{162}, \fpage{1438}, \doi{10.1016/j.renene.2020.08.001}</r>

12. <r>\author{<a><g>W.</g><s>Peng</s><a><g>Z. S.</g><s>Ye</s><a><g>N.</g><s>Chen</s>}, \title{Bayesian deep-learning-based health prognostics toward prognostics uncertainty}, \journal{IEEE Trans. Ind. Electron.}, \year{2019}, \vol{67}, \fpage{2283}, \doi{10.1109/TIE.2019.2907440}</r>

13. <r>\author{<a><g>J.</g><s>Liu</s><a><g>K.</g><s>Pan</s>}, \title{Rigid-flexible-thermal coupling dynamic formulation for satellite and plate multibody system}, \journal{Aerosp. Sci. Tech.}, \year{2016}, \vol{52}, \fpage{102}, \doi{10.1016/j.ast.2016.02.025}</r>

14. <r>\author{<a><g>Z.</g><s>Shen</s><a><g>Q.</g><s>Tian</s><a><g>X.</g><s>Liu</s><a><g>G.<

/g><s>Hu</s>}, \title{Thermally induced vibrations of flexible beams using Absolute Nodal Coordinate Formulation}, \journal{Aerosp. Sci. Tech.}, \year{2013}, \vol{29}, \fpage{386}, \doi{10.1016/j.ast.2013.04.009}</r>

15. <r>\author{<a><g>S.</g><s>Pandey</s><a><g>S.</g><s>Pradyumna</s>}, \title{A finite element formulation for thermally induced vibrations of functionally graded material sandwich plates and shell panels}, \journal{Compos. Struct.}, \year{2017}, \vol{160}, \fpage{877}, \doi{10.1016/j.compstruct.2016.10.040}</r>

16. <r>\author{<a><g>L.</g><s>Coox</s><a><g>F.</g><s>Greco</s><a><g>O.</g><s>Atak</s><a><g>D.</g><s>Vandepitte</s><a><g>W.</g><s>Desmet</s>}, \title{A robust patch coupling method for NURBS-based isogeometric analysis of non-conforming multipatch surfaces}, \journal{Comput. Methods Appl. Mech. Eng.}, \year{2017}, \vol{316}, \fpage{235}, \doi{10.1016/j.cma.2016.06.022}, \ads{2017CMAME.316..235C}</r>

17. <r>J. A. Cottrell, T. J. Hughes, and Y. Bazilevs, Isogeometric analysis: toward integration of CAD and FEA (John Wiley & Sons, 2009)</r>

18. <r>\author{<a><g>Z. P.</g><s>Wang</s><a><g>S.</g><s>Turteltaub</s><a><g>M.</g><s>Abdalla</s>}, \title{Shape optimization and optimal control for transient heat conduction problems using an isogeometric approach}, \journal{Comput. Struct.}, \year{2017}, \vol{185}, \fpage{59}, \doi{10.1016/j.compstruc.2017.02.004}</r>

19. <r>\author{<a><g>T. A.</g><s>Huynh</s><a><g>X. Q.</g><s>Lieu</s><a><g>J.</g><s>Lee</s>}, \title{NURBS-based modeling of bidirectional functionally graded Timoshenko beams for free vibration problem}, \journal{Compos. Struct.}, \year{2017}, \vol{160}, \fpage{1178}, \doi{10.1016/j.compstruct.2016.10.076}</r>

20. <r>\author{<a><g>H. S.</g><s>Yang</s><a><g>C. Y.</g><s>Dong</s>}, \title{Adaptive extended isogeometric analysis based on PHT-splines for thin cracked plates and shells with Kirchhoff-Love theory}, \journal{Appl. Math. Model.}, \year{2019}, \vol{76}, \fpage{759}, \doi{10.1016/j.apm.2019.07.002}</r>

21. <r>\author{<a><g>H.</g><s>Li</s><a><g>H.</g><s>Diaz</s><a><g>C.</g><s>Guedes Soares</s>}, \title{A developed failure mode and effect analysis for floating offshore wind turbine support structures}, \journal{Renew. Energy}, \year{2021}, \vol{164}, \fpage{133}, \doi{10.1016/j.renene.2020.09.033}</r>

22. <r>\author{<a><g>M. A.</g><s>Hariri-Ardebili</s><a><g>S.</g><s>Mahdi Seyed-Kolbadi</s><a><g>V. E.</g><s>Saouma</s><a><g>J. W.</g><s>Salamon</s><a><g>L. K.</g><s>Nuss</s>}, \title{Anatomy of the vibration characteristics in old arch dams by random field theory}, \journal{Eng. Struct.}, \year{2019}, \vol{179}, \fpage{460}, \doi{10.1016/j.engstruct.2018.10.082}</r>

23. <r>\author{<a><g>G.</g><s>Stefanou</s>}, \title{The stochastic finite element method: past, present and future}, \journal{Comput. Methods Appl. Mech. Eng.}, \year{2009}, \vol{198}, \fpage{1031}, \doi{10.1016/j.cma.2008.11.007}, \ads{2009CMAME.198.1031S}</r>

24. <r>\author{<a><g>J.</g><s>Ma</s><a><g>J.</g><s>Chen</s><a><g>Y.</g><s>Xu</s><a><g>T.</g><s>Jiang</s>}, \title{Dynamic characteristic analysis of fuzzy-stochastic truss structures based on fuzzy factor method and random factor method}, \journal{Appl. Math. Mech.}, \year{2006}, \vol{27}, \fpage{823}, \doi{10.1007/s10483-006-0613-z}</r>

25. <r>\author{<a><g>C.</g><s>Nastos</s><a><g>D.</g><s>Zarouchas</s>}, \title{Probabilistic failure

analysis of quasi-isotropic CFRP structures utilizing the stochastic finite element and the Karhunen-Loève expansion methods}, \journal{Compos. Part B-Eng.}, \year{2022}, \vol{235}, \fpage{109742}, \doi{10.1016/j.compositesb.2022.109742}</r>

26. <r>\author{<a><g>J.</g><s>Ma</s><a><g>B.</g><s>Liu</s><a><g>P.</g><s>Wriggers</s><a><g>W.</g><s>Gao</s><a><g>B.</g><s>Yan</s>}, \title{The dynamic analysis of stochastic thin-walled structures under thermal-structural-acoustic coupling}, \journal{Comput. Mech.}, \year{2020}, \vol{65}, \fpage{609}, \doi{10.1007/s00466-019-01786-0}, \ads{2019CompM..65..609M}</r>

27. <r>\author{<a><g>J. D.</g><s>Arregui-Mena</s><a><g>L.</g><s>Margetts</s><a><g>P. M.</g><s>Mummery</s>}, \title{Practical application of the stochastic finite element method}, \journal{Arch. Computat. Methods Eng.}, \year{2016}, \vol{23}, \fpage{171}, \doi{10.1007/s11831-014-9139-3}</r>

28. <r>\author{<a><g>C.</g><s>Scarth</s><a><g>S.</g><s>Adhikari</s><a><g>P. H.</g><s>Cabral</s><a><g>G. H. C.</g><s>Silva</s><a><g>A. P.</g><s>Prado</s>}, \title{Random field simulation over curved surfaces: Applications to computational structural mechanics}, \journal{Comput. Methods Appl. Mech. Eng.}, \year{2019}, \vol{345}, \fpage{283}, \doi{10.1016/j.cma.2018.10.026}, \ads{2019CMAME.345..283S}</r>

29. <r>\author{<a><g>G.</g><s>Stefanou</s><a><g>D.</g><s>Savvas</s><a><g>M.</g><s>Papadrakakis</s>}, \title{Stochastic finite element analysis of composite structures based on material microstructure}, \journal{Compos. Struct.}, \year{2015}, \vol{132}, \fpage{384}, \doi{10.1016/j.compstruct.2015.05.044}</r>

30. <r>\author{<a><g>W.</g><s>Betz</s><a><g>I.</g><s>Papaioannou</s><a><g>D.</g><s>Straub</s>}, \title{Numerical methods for the discretization of random fields by means of the Karhunen-Loève expansion}, \journal{Comput. Methods Appl. Mech. Eng.}, \year{2014}, \vol{271}, \fpage{109}, \doi{10.1016/j.cma.2013.12.010}, \ads{2014CMAME.271..109B}</r>

31. <r>\author{<a><g>M. L.</g><s>Mika</s><a><g>T. J. R.</g><s>Hughes</s><a><g>D.</g><s>Schillinger</s><a><g>P.</g><s>Wriggers</s><a><g>R. R.</g><s>Hiemstra</s>}, \title{A matrix-free isogeometric Galerkin method for Karhunen–Loève approximation of random fields using tensor product splines, tensor contraction and interpolation based quadrature}, \journal{Comput. Methods Appl. Mech. Eng.}, \year{2021}, \vol{379}, \fpage{113730}, \doi{10.1016/j.cma.2021.113730}, \ads{2021CMAME.379k3730M}</r>

32. <r>\author{<a><g>K. K.</g><s>Phoon</s><a><g>S. P.</g><s>Huang</s><a><g>S. T.</g><s>Quek</s>}, \title{Simulation of second-order processes using Karhunen-Loeve expansion}, \journal{Comput. Struct.}, \year{2002}, \vol{80}, \fpage{1049}, \doi{10.1016/S0045-7949(02)00064-0}</r>

33. <r>\author{<a><g>R.</g><s>Echter</s><a><g>M.</g><s>Bischoff</s>}, \title{Numerical efficiency, locking and unlocking of NURBS finite elements}, \journal{Comput. Methods Appl. Mech. Eng.}, \year{2010}, \vol{199}, \fpage{374}, \doi{10.1016/j.cma.2009.02.035}, \ads{2010CMAME.199..374E}</r>

34. <r>\author{<a><g>N.</g><s>Vu-Bac</s><a><g>T. X.</g><s>Duong</s><a><g>T.</g><s>Lahmer</s><a><g>X.</g><s>Zhuang</s><a><g>R. A.</g><s>Sauer</s><a><g>H. S.</g><s>Park</s><a><g>T.</g><s>Rabczuk</s>}, \title{A

NURBS-based inverse analysis for reconstruction of nonlinear deformations of thin shell structures}, \journal{Comput. Methods Appl. Mech. Eng.}, \year{2018}, \vol{331}, \fpage{427}, \doi{10.1016/j.cma.2017.09.034}, \ads{2018CMAME.331..427V}, \arxiv{1902.02204}</r>

35. <r>Y. Otoguro, T. Kenji, and E. T. Tayfun, in A general-purpose NURBS mesh generation method for complex geometries: Proceedings of Frontiers in Computational Fluid-Structure Interaction and Flow Simulation, Birkhäuser, Cham, 2018, pp. 399-434</r>

36. <r>\author{<a><g>S.</g><s>Faroughi</s><a><g>E.</g><s>Shafei</s><a><g>A.</g><s>Eriksson</s>}, \title{NURBS-based modeling of laminated composite beams with isogeometric displacement-only theory}, \journal{Compos. Part B-Eng.}, \year{2019}, \vol{162}, \fpage{89}, \doi{10.1016/j.compositesb.2018.10.073}</r>

37. <r>\author{<a><g>C. L.</g><s>Thanh</s><a><g>L. V.</g><s>Tran</s><a><g>T. Q.</g><s>Bui</s><a><g>H. X.</g><s>Nguyen</s><a><g>M.</g><s>Abdel-Wahab</s>}, \title{Isogeometric analysis for size-dependent nonlinear thermal stability of porous FG microplates}, \journal{Compos. Struct.}, \year{2019}, \vol{221}, \fpage{110838}, \doi{10.1016/j.compstruct.2019.04.010}</r>

38. <r>\author{<a><g>L.</g><s>Coradello</s><a><g>P.</g><s>Antolin</s><a><g>R.</g><s>Vázquez</s><a><g>A.</g><s>Buffa</s>}, \title{Adaptive isogeometric analysis on two-dimensional trimmed domains based on a hierarchical approach}, \journal{Comput. Methods Appl. Mech. Eng.}, \year{2020}, \vol{364}, \fpage{112925}, \doi{10.1016/j.cma.2020.112925}, \ads{2020CMAME.364k2925C}, \arxiv{1910.03882}</r>

39. <r>\author{<a><g>D.</g><s>Roy</s><a><g>M. K.</g><s>Dash</s>}, \title{Explorations of a family of stochastic Newmark methods in engineering dynamics}, \journal{Comput. Methods Appl. Mech. Eng.}, \year{2005}, \vol{194}, \fpage{4758}, \doi{10.1016/j.cma.2004.11.010}, \ads{2005CMAME.194.4758R}</r>

40. <r>\author{<a><g>S.</g><s>Gao</s><a><g>F.</g><s>Liu</s><a><g>S.</g><s>Chang</s><a><g>L.</g><s>Zhou</s>}, \title{A dynamic response analysis method with high-order accuracy for fixed offshore structures based on a normalised expression of external loadings}, \journal{Ocean Eng.}, \year{2021}, \vol{219}, \fpage{108358}, \doi{10.1016/j.oceaneng.2020.108358}</r>

41. <r>\author{<a><g>Y.</g><s>Wu</s><a><g>H.</g><s>Wang</s><a><g>J.</g><s>Liu</s><a><g>S.</g><s>Zhang</s><a><g>H.</g><s>Huang</s>}, \title{A novel dynamic isogeometric reanalysis method and its application in closed-loop optimization problems}, \journal{Comput. Methods Appl. Mech. Eng.}, \year{2019}, \vol{353}, \fpage{1}, \doi{10.1016/j.cma.2019.04.039}, \ads{2019CMAME.353....1W}</r>